ACS OMEGA

http://pubs.acs.org/journal/acsodf

Article

Green Synthesis of Silver Nanoparticles Using the *Lotus lalambensis* Aqueous Leaf Extract and Their Anti-Candidal Activity against Oral Candidiasis

Basem M. Abdallah* and Enas M. Ali

Cite This: *ACS Omega* 2021, 6, 8151−8162

Read Online

ACCESS | Metrics & More | Article Recommendations

ABSTRACT: Oral candidiasis is widely spread in both humans and animals, which is caused mainly by *Candida albicans*. In this study, we aimed to biosynthesize silver nanoparticles (AgNPs) for the first time using the *Lotus lalambensis* Schweinf leaf extract (L-AgNPs) and investigated their anti-candidal potency alone or in combination with the leaf extract of *L. lalambensis* (L-AgNPs/LL) against *C. albicans*. The biosynthesized L-AgNPs were characterized by imaging (transmission electron microscopy, TEM), UV−vis spectroscopy, Fourier transform infrared spectroscopy (FTIR), and X-ray diffraction (XRD). The results of the disk diffusion method showed the potent synergistic anti-candidal activity of L-AgNPs/LL (24 mm inhibition zone). L-AgNPs/LL completely inhibited the morphogenesis of *C. albicans* and suppressed the adhesion and the formation of the biofilm of *C. albicans* by 82.5 and 78.7%, respectively. Further, L-AgNPs/LL inhibited the production of antioxidant enzymes of *C. albicans* by 80%. SEM and TEM revealed deteriorations in the cell wall ultrastructure in L-AgNPs/LL-treated *C. albicans*. Interestingly, L-AgNPs/LL showed less than 5% cytotoxicity when examined with either the primary bone marrow derived mesenchymal stem cell (BMSCs) or MCF-7 cell line at MIC values of L-AgNPs/LL. In conclusion, we identified L-AgNPs/LL as a potential biosynthesized-based drug for oral candidiasis in humans and animals.

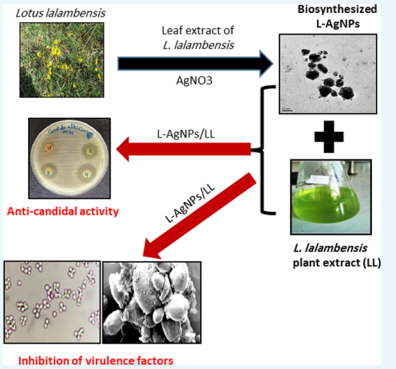

1. INTRODUCTION

The oral cavity is one of the most complex cavities of the human body, comprising hundreds of different bacterial, viral, and fungal species.[1] The most prevalent *Candida* species recovered from the human mouth, in both the commensal state and cases of oral candidiasis, is *Candida albicans*.[2] Additionally, *C. albicans* infection is widely distributed in animals, including all domestic animals like cattle, horses, pigs, cats, and dogs as well as birds.[3,4] In wild animals, candidiasis affects the mucous membranes and the skin causing ulcers and whitish streaks and plaques on the tongue, oral cavity, and esophagus.[5] For example, in camels, candidiasis affects the mucous membranes and the skin,[6] and in dogs, candidiasis is clinically demonstrated as seborrheic dermatitis, alopecia, patchy erythema, and superficial erosions.[7] Several predisposing factors were found to cause oral candidiasis including chemotherapy, immunosuppressive conditions, mucosal injuries, and deceased salivary flow.[8] Virulence attributes controlling the infection capacity of *C. albicans* include the dimorphic morphogenesis between yeast and filamentous forms (morphogenesis). The formation of biofilms also acts as a key factor in infection as cells in the biofilm show greater resistance to antimicrobial agents due to the inadequate penetration of antifungals.[9]

Treatments of oral candidiasis usually involve the use of topical or systemic antifungal drugs and denture cleansers in the case of denture stomatitis.[10] However, these agents have several adverse health effects.[11] Compared to antibiotics, currently available antifungal drugs are limited and their production without toxicity is very complicated due to the eukaryotic nature of *Candida*.[12] The continuous emergence of *Candida* strains resistant to currently available antifungal drugs demands the development of novel alternatives drugs. In this context, natural antifungal drugs including plant-derived alcoholic extracts and essential oils were used as antifungal agents against *C. albicans*.[13−15] In addition, AgNPs were efficiently used for the treatment of candidiasis.[16−19] AgNPs were found to exert a high capacity to anchor to cell wall of *C. albicans*, then penetrating it, resulting in structural alterations in the integrity of the plasma membrane.[20] Plant-mediated synthesis of AgNPs has acquired great attention due to its lower toxicity, cost efficiency, eco-friendliness, and low time of

Received: December 10, 2020
Accepted: March 8, 2021
Published: March 15, 2021

https://dx.doi.org/10.1021/acsomega.0c06009
ACS Omega 2021, 6, 8151−8162

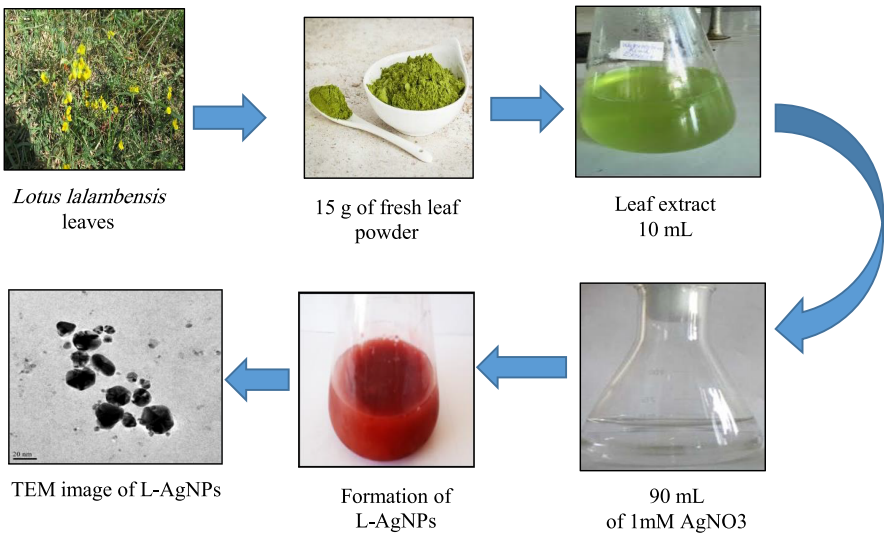

Figure 1. Biosynthesis of L-AgNPs using the *L. lalambensis* Schweinf leaf extract. The leaf extract of *L. lalambensis* was used to function as the biocatalyst for the reduction of silver ions to silver, as shown by the change in color from light yellow to dark brown. L-AgNPs were synthesized by treating the leaf extract with 1 mM $AgNO_3$ solution at 27 °C under dark conditions. TEM shows the size and morphology of monodisperse L-AgNPs ranging from 6 to 26 nm.

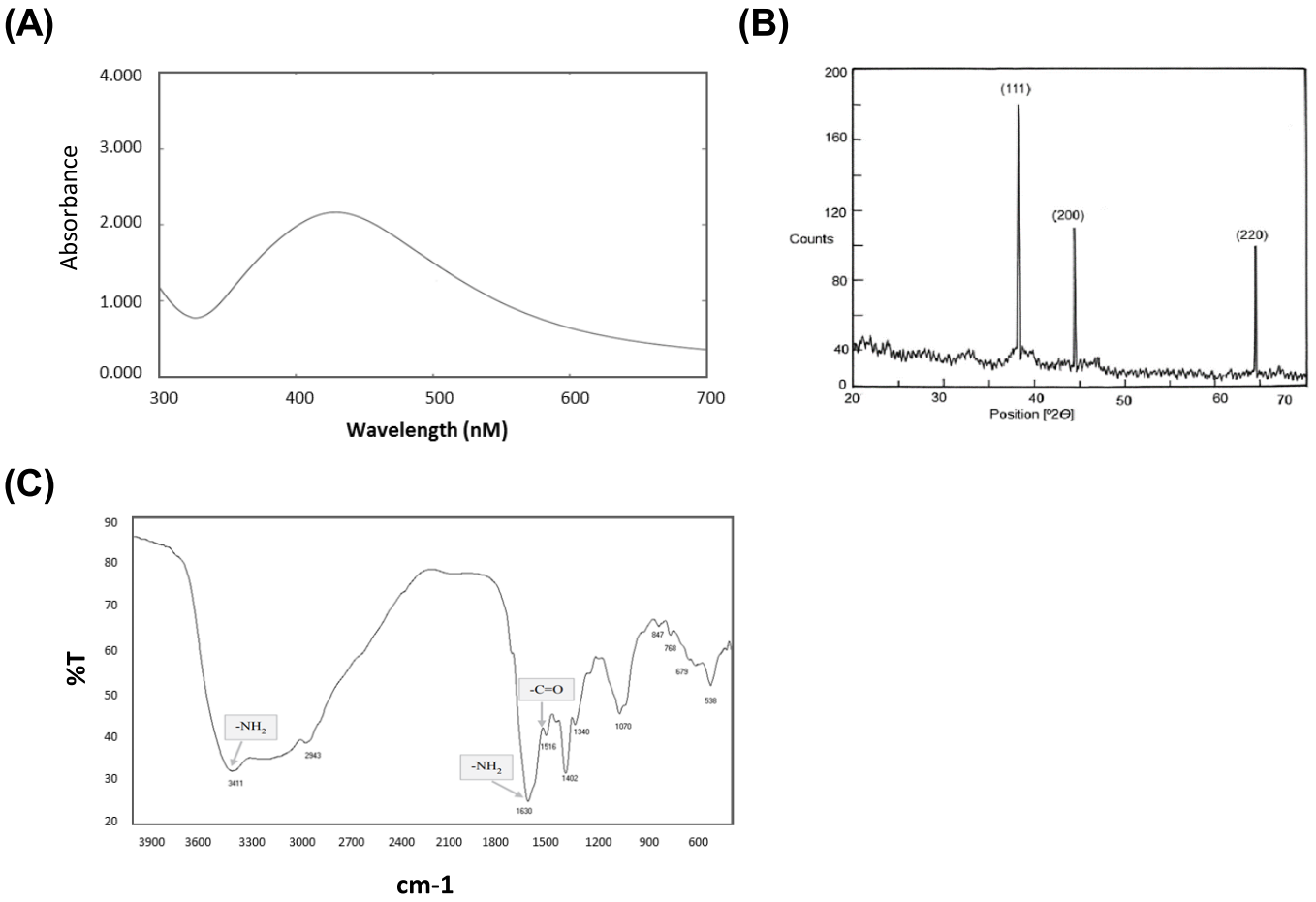

Figure 2. Confirmation of biosynthesized L-AgNPs. (A) UV−vis spectrum of L-AgNPs. The values of peaks for the UV−vis were plotted between AgNPs/absorbance ratios. The maximum absorbance peak was at around 450 nm, consistent with the surface plasmon resonance of AgNPs. (B) XRD for L-AgNPs displayed three different diffraction bands at 38.18, 44.35, and 64.4° indexed 2θ (degree) values of the (111), (200), and (220) crystalline planes of cubic Ag. (C) FTIR of L-AgNPs showing amide I (−C=O) and amide II (−NH) bands.

consumption.[21] Additionally, plants are good and easily available sources for biologically active secondary metabolites, which can act as reducing, stabilizing, and capping agents in the reduction of silver ions to AgNPs, resulting in the production of nanoparticles with lesser toxicity over chemical and physical synthesis methods.[22,23] Chemical synthesis

https://dx.doi.org/10.1021/acsomega.0c06009
ACS Omega 2021, 6, 8151−8162

methods resulted in the production of toxic compounds, which can limit the use of AgNPs in medical applications, while physical synthesis methods are time-consuming processes that produce nonuniform nanoparticles.[24] In this context, we have recently demonstrated the effective inhibition of candidiasis using AgNPs biosynthesized from the *Calotropis gigantea* leaf extract.[19]

The genus *Lotus*, belonging to the family Fabaceae, contains more than 100 species distributed all over the world, particularly around the Mediterranean region. In traditional medicine, plants of the genus *Lotus* are used as antimicrobials, contraceptives, and prophylactics and for treatment of sexually transmitted diseases.[25,26] *L. lalambensis* Schweinf is one species of the genus *Lotus* that is enriched with several biological active secondary metabolites.[27] We have recently extracted and purified 5′-hydroxy auraptene (5′-HA) from *L. lalambensis*, with potent antifungal and anti-mycotoxigenic potentials against *Aspergillus flavus*.[28] In addition, we identified 5′-HA as a plausible drug for osteoporosis that acts to promote osteogenesis and inhibit osteoclastogenesis.[29,30] Thus, we aimed to use *L. lalambensis* for the biosynthesis of AgNPs (L-AgNPs). Our results demonstrated the synergism of the antifungal effect of L-AgNPs in combination with the leaf extract of *L. lalambensis* (L-AgNPs/LL) against oral candidiasis. This effect was shown to be through the inhibition of growth, dimorphic transition, and formation of the biofilm without signs of cytotoxicity in animal cells.

2. RESULTS

2.1. Biosynthesis and Characterization of F-AgNPs. L-AgNPs were biosynthesized from an aqueous leaf extract of *L. lalambenesis*. The capability of the biologically active constituents of the extract to act as biocatalysts for the reduction of silver ions to silver was assessed. The color change of the extract of *L. lalambenesis* after addition of $AgNO_3$ from colorless to brown was detected (Figure 1). This brown color indicated the AgNP formation. The synthesis of L-AgNPs was confirmed by TEM, which shows that the morphology of the L-AgNPs is nearly spherical. The particle size ranges from 6 to 26 nm having a size of about 16.7 nm (Figure 1).

UV−visible spectrophotometry was carried out, and the spectrum displays surface plasmon resonance at the 422 nm absorption band (Figure 2A). The color of the solution was characteristic to the absorption wavelength in the visible region. The XRD displayed a diffraction line at low angles (30−80°). The Bragg reflections at angles 2θ of 38.18, 44.35, 64.4, and 77.3° matched with the 111, 200, 220, and 311 bands, respectively (Figure 2B). This configuration confirmed the structure of L-AgNPs as a cubic structure. XRD confirmed the crystalline structure of the silver in the *L. lalambenesis* leaf extract. The FTIR spectrum of L-AgNPs showed 11 peaks: 538, 679, 768, 847, 1070, 1340, 1432, 1516, 1630, 2943, and 3411 cm^{-1} in the region of 500−400 cm^{-1} (Figure 2C). The band at 1630 cm^{-1} corresponds to the stretching vibration of −C=O (carbonyl), which is identified as the amide I band, while the bands at 3411 and 1516 cm^{-1} characterize the stretching and bending vibrations of −NH, respectively. Last, TEM gave further evidence about the shape, size, and distribution profile of the biosynthesized L-AgNPs.

2.2. Synergistic Anti-Candidal Action of L-AgNPs/LL. We investigated the anti-candidal potential of the plant extract, L-AgNPs and L-AgNPs/LL using a disk diffusion method. The L-AgNPs displayed a higher anti-candidal action where the diameter of the inhibition zone (IZD) was 19 mm, although the extract showed moderate anti-candidal potential with an IZD of 15 mm (Table 1 and Figure 3A). The MIC values of L-AgNPs and plant extract were 50 and 100 μg/mL, respectively (Table 1). L-AgNPs/LL displayed synergistic anti-candidal potential against *C. albicans*, with a zone of inhibition of 24 mm (Figure 3A). Additionally, the time-kill curves showed the fungistatic action of both L-AgNPs and plant extract at 50 and 100 μg/mL, respectively, on the growth of *Candida* cells (Figure 3B). After 4 h of incubation, L-AgNPs/LL completely repressed the growth of *C. albicans* (Figure 3B). Thus, L-AgNPs/LL exhibited a greater anti-candidal action than either the L-AgNPs or the plant extract.

Table 1. Anti-Candidal Action of L-AgNPs and *L. lalambenesis* Extract against *C. albicans*[a]

	antifungal agent		
	DMSO	plant extract	L-AgNPs
concentration (μg/mL)		IZD (mm)	
0	$_a0^a \pm 0.0$	$_a0^a \pm 0.0$	$_a0^a \pm 0.0$
6.25	$_a0^a \pm 0.0$	$_b2^b \pm 0.7$	$_b10^c \pm 0.7$
12.5	$_a0^a \pm 0.0$	$_c4^b \pm 0.5$	$_c13^c \pm 0.5$
25	$_a0^a \pm 0.0$	$_d7^b \pm 0.5$	$_d16^c \pm 0.8$
50	$_a0^a \pm 0.0$	$_e10^b \pm 0.5$	$_e19^c \pm 0.8$
100	$_a0^a \pm 0.0$	$_f15^b \pm 0.5$	no growth
200	$_a0^a \pm 0.0$	no growth	
400	$_a0^a \pm 0.0$		

[a]IZD = inhibition zone diameter (mm). Data are presented as the mean of the zone of inhibition in mm followed by SD. The values with different subscript letters in the same column and those with different subscript letters in the same row are significantly different according to ANOVA and Duncan's multiple range tests.

2.3. L-AgNPs/LL Inhibits the Virulence Factors of *C. albicans*. The untreated control (DMSO) of *C. albicans* exhibited excessive hyphal growth after 6 h, whereas the morphological transition of *C. albicans* was inhibited by L-AgNPs at concentrations lower than the MIC (25 μg/mL). Hyphal growth was completely blocked in the presence of L-AgNPs/LL (50/100 μg/mL), as evaluated by phase contrast microscopic observations (Figure 4A and Table 2). Additionally, we studied the anti-adhesive and anti-biofilm effectiveness of the L-AgNPs. L-AgNPs (50 μg/mL) repressed the adhesion and the growth of the biofilm of *C. albicans* by 74.2 and 64.6%, respectively, while L-AgNPs/LL repressed the adhesion and biofilm formation of *C. albicans* by 89.7 and 79.1%, respectively (Figure 4B,C).

2.4. L-AgNPs/LL Suppresses the Production of Oxidative Enzymes by *C. albicans*. Since very limited data are available about the suppression of the production of antioxidant enzymes by nanoparticles, we assessed the effect of L-AgNPs/LL on the production of oxidative enzymes by *C. albicans*. Remarkably, L-AgNPs/LL suppresses the following antioxidant-related enzymes GST, CAT, SOD, G6-P, GSR, and GPX by 88.13, 76.15, 95.46, 87.69, 85.7, and 85.52%, respectively, in *C. albicans* (Table 3).

2.5. L-AgNPs/LL Increases the Intracellular Glucose and Trehalose Release. *C. albicans* were cultured in the presence of the plant extract, L -AgNPs, and L-AgNPs/LL, and the amounts of released glucose and trehalose were measured. Cells treated with either the plant extract or L-AgNPs

https://dx.doi.org/10.1021/acsomega.0c06009
ACS Omega 2021, 6, 8151−8162

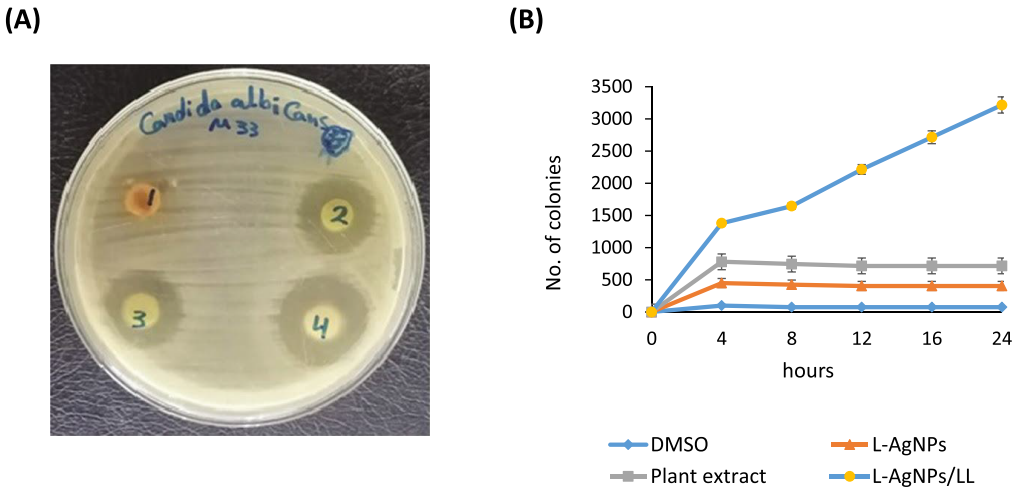

Figure 3. Antimicrobial potential of L-AgNPs and L-AgNPs/LL (A) Disk diffusion method displaying the anti-candidal action of (1) DMSO, (2) plant extract (100 μg/mL), (3) L-AgNPs (50 μg/mL), and (4) L-AgNPs/LL (50/100 μg/mL). (B) Time-kill assay of the effect of the plant extract (100 μg/mL), L-AgNPs (50 μg/mL), and L-AgNPs/LL (50/100 μg/mL) on *Candida* cells. *Candida* cells treated with DMSO were used as a control.

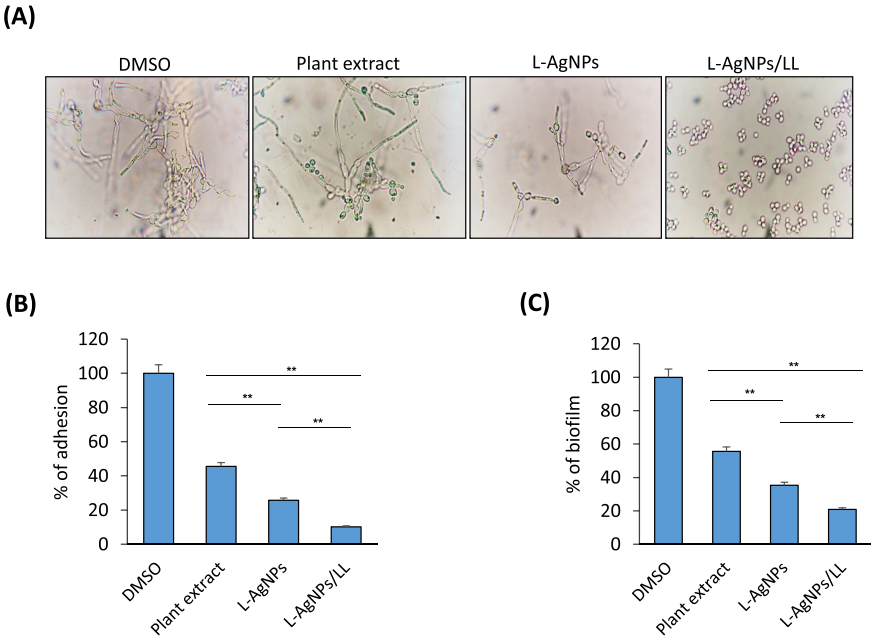

Figure 4. Effect of L-AgNPs and L-AgNPs/LL on virulence factors of *C. albicans*. (A) Dimorphic transition; (B) adhesion after (2 h). (C) Biofilm formation (after 24 h); complete repression of the morphological transition, biofilm, and adhesion of *C. albicans* was observed when L-AgNPs and *L. lalambenesis* extract were mixed, not like when the two were used separately. Values are mean ± SD of three independent experiments (**p < 0.005(.

accumulated more intracellular glucose and trehalose than DMSO-treated cells (control). Additionally, these cells also have increased more extracellular glucose and trehalose than DMSO-treated cells (Figure 5A,B). Interestingly, the highest induction of extracellular glucose and trehalose was brought by L-AgNPs/LL, which was measured to be 45.2 μg per fungal dry weight of 1 mg (Figure 5B). This rate was significantly higher than those induced in either the plant extract or L-AgNPs (31.9 and 27.5 μg/mg, respectively).

2.6. Ultrastructural Examination of the Interaction between AgNPs and *C. albicans* Cells Using SEM and TEM. To examine the effect of the plant extract, L-AgNPs, and L-AgNPs/LL on the morphology and ultrastructure of *C. albicans*, scanning and transmission electron microscopy techniques were used. Our results showed that *C. albicans* treated with L-AgNPs/LL underwent noticeable morphological changes. In cells treated with L-AgNPs or plant extract, yeast agglutination was observed, while in cells treated with L-AgNPs/LL, a material deposited on the cell walls of *C. albicans* was detected (Figure 6A). The results of TEM showed that DMSO-treated *C. albicans* cells (control) displayed a normal intramorphological structure with several organelles of *Candida* cells surrounded by the cytoplasm. The plasma membrane and cell wall have a uniform thickness. Nevertheless, plant-extract-treated cells showed that there were alterations in the morphological structures of the cells, which cause lysis. Some organelles such as the nucleus and vacuole disappeared. The plant extract has changed the cytoplasm of *C. albicans* cells

https://dx.doi.org/10.1021/acsomega.0c06009
ACS Omega 2021, 6, 8151−8162

Table 2. Effect of L-AgNPs, Plant Extract, and L-AgNPs/LL on the Dimorphic Transition of *C. albicans*[a]

antifungal agent	YF count (cell/mL)	FF count (cell/mL)	% of dimorphism
DMSO	$66^{b} \pm 4.0$	$1820^{d} \pm 4.0$	96.37 ± 1.5
plant extract	$510^{d} \pm 6.0$	$920^{c} \pm 2.0$	44.56 ± 1.1
L-AgNPs	$266^{c} \pm 5.0$	$383^{b} \pm 1.5$	30.45 ± 0.9
L-AgNPs/LL	$10^{a} \pm 2.5$	$12^{a} \pm 0.76$	16.66 ± 0.8

[a]Results are presented as the mean of the inhibition zone (mm) followed by SD. The values with different subscript letters in the same column and those with different subscript letters in the same row are significantly different according to ANOVA and Duncan's multiple range tests. YF: yeast form. FF: filamentous form. % of dimorphism = FF − YF/FF × 100.

Table 3. Specific Activities of Antioxidant Enzymes

		specific activity (U/mg protein)	
enzyme	substrate	control	L-AgNPs/LL
glutathione-S transferase	CDNB	0.633 ± 0.11	0.0751 ± 0.002
catalase	H_2O_2	3.9 ± 0.33	0.93 ± 0.11
superoxide dismutase	epinephrine	0.708 ± 0.06	0.0321 ± 0.012
glucose 6 phosphate dehydrogenase	NADP	635.24 ± 5.11	78.14 ± 1.3
glutathione reductase	NADPH	75.22 ± 2.13	9.33 ± 0.37
glutathione peroxidase	NADPH	0.00076 ± 0.0001	0.00011 ± 0.0

when compared to the control cells. L-AgNPs-treated *C. albicans* cells exhibited great modification of the organelles. Impartiality of the cell membrane from the cell wall and formation of pores were observed, which resulted in the leakage of cell contents. Additionally, the disorganization of the cell wall and disruption of the cell membrane were noticed. Importantly, L-AgNPS/LL-treated cells showed perturbation of the cell wall, disruption of the cell membrane, and formation of pores with a complete collapse of the cells. The shrinkage of the cytoplasm from the cell wall was observed. The leakage of the intracellular contents from the cells was more pronounced, which finally led to cell death (Figure 6B).

2.7. L-AgNPs/LL Does Not Show any Cytotoxicity with Animal Cell Lines. As a prerequisite step for the preclinical study of L-AgNPs/LL in the oral candidiasis animal model, we examined the cytotoxicity of the plant extract, L-AgNPs, and L-AgNPs/LL on both primary mouse BMSCs and MCF-7 cell line using the cell viability MTT assay. As shown in Figure 7A,B, plant extracts were not toxic to mBMSCs and MCSF-7 up to a concentration of 200 μg/mL. The cytotoxicity of L-AgNPs alone revealed significant reduction in cell viability at a concentration above 50 μg/mL (Figure 7A,B). Accordingly, L-AgNPs/LL showed cytotoxicity at a concentration above 50/100 μg/mL of L-AgNPs/LL (Figure 7A,B). These preliminary data demonstrated that the concentration of L-AgNPs/LL (50/100 μg/mL) is safe to use *in vivo* as a promising anti-candidiasis drug.

3. DISCUSSION

The development of reliable, eco-friendly approaches for the production of nanoparticles is a key aspect of nanotechnology nowadays. In this study, we were the first to use *L. lalambensis* in the biosynthesis of AgNPs.

In our study, the formation of a brown color in a solution containing the aqueous leaf extract is evidence for the synthesis of L-AgNPs in the reaction mixture and is a main cause of the excitation of surface plasmon vibrations in the nanoparticles.[31,32] UV analysis demonstrated the SPR absorption of our L-AgNPs at 422 nm as described previously for AgNPs.[33,34] The particle sizes of our L-AgNPs ranged from 6 to 26 nm. FTIR was performed to recognize the biomolecules accountable for the capping and effective stabilization of the metal nanoparticles and to realize the protein−metal nanoparticle interaction. Our FTIR spectrum demonstrated the presence of amide I and amide II bands obtained due to the carbonyl stretch and −N−H stretch vibrations in the amide linkage of the protein, suggesting that the protein molecules can also act as stabilizing agents by binding the AgNPs through free amino groups as described previously.[35]

Our results identified the MIC for L-AgNPs to be 50 μg/mL with a high anti-candidal activity. This might be attributed to the presence of tannins, coumarins, and flavonoids in the whole extract.[36] In this context, synthesized AgNPs using the extract of *Lycopersicon esculentum* displayed inhibitory action

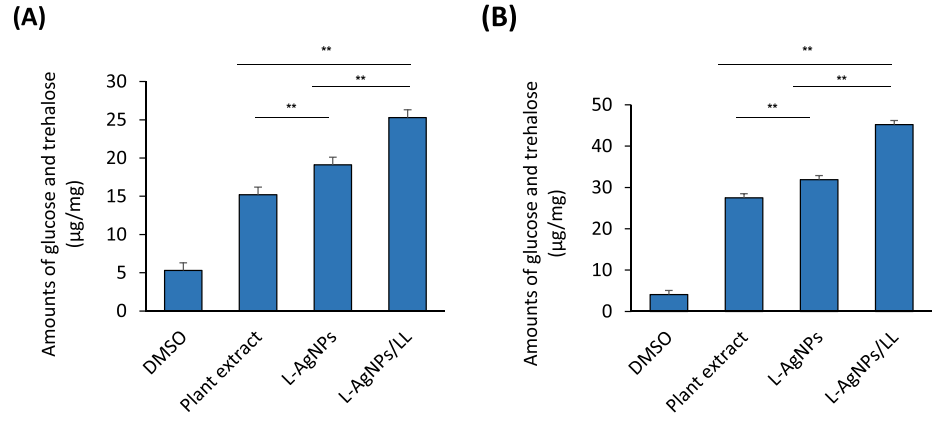

Figure 5. Effect of L-AgNPs and L-AgNPs/LL on the intracellular glucose and trehalose release. (A) The concentrations of intracellular and (B) extracellular trehalose and glucose from *C. albicans* by the plant extract (100 μg/mL), L-AgNPs (50 μg/mL), and L-AgNPs/LL (50/100 μg/mL). *C. albicans* was mixed with 0.05 units of trehalase and 16% DNS reagent. The enzymatic reaction was carried out for 1 h at 37 °C. Color formations were measured at 525 nm. Values are mean ± SD of three independent experiments (**p < 0.005(.

https://dx.doi.org/10.1021/acsomega.0c06009
ACS Omega 2021, 6, 8151−8162

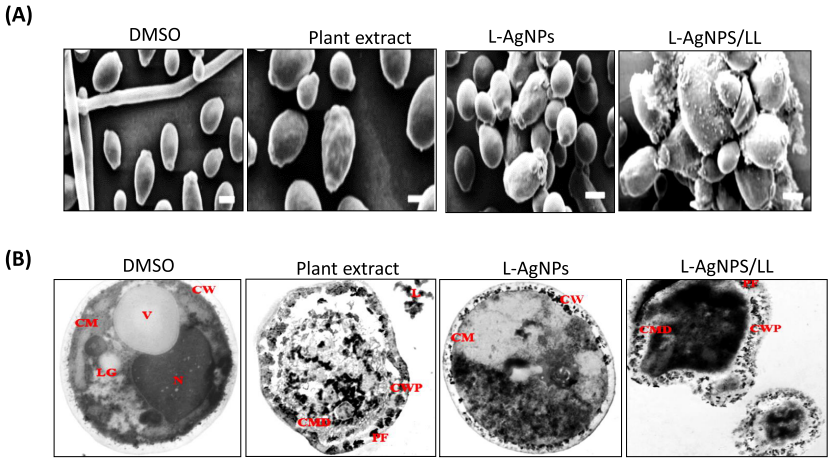

Figure 6. Electron microscopy photographs of *C. albicans*. (A) TEM photographs of *C. albicans* treated with the plant extract (100 μg/mL), L-AgNPs (50 μg/mL), and L-AgNPs/LL (50/100 μg/mL). Bar = 2 mm. (B) SEM of a *C. albicans* treated with the plant extract, L-AgNPs, and L-AgNPs/LL. 6300× magnification was used for all images. Bar = 1 μm. CM: cell membrane; CMD: cell membrane disruption; CW: cell wall; CWP: Cell wall perturbation; L: leakage; LG: lipid granule; N: nucleus; NC: nanocapsule; PF: pore formation; V: vacuole.

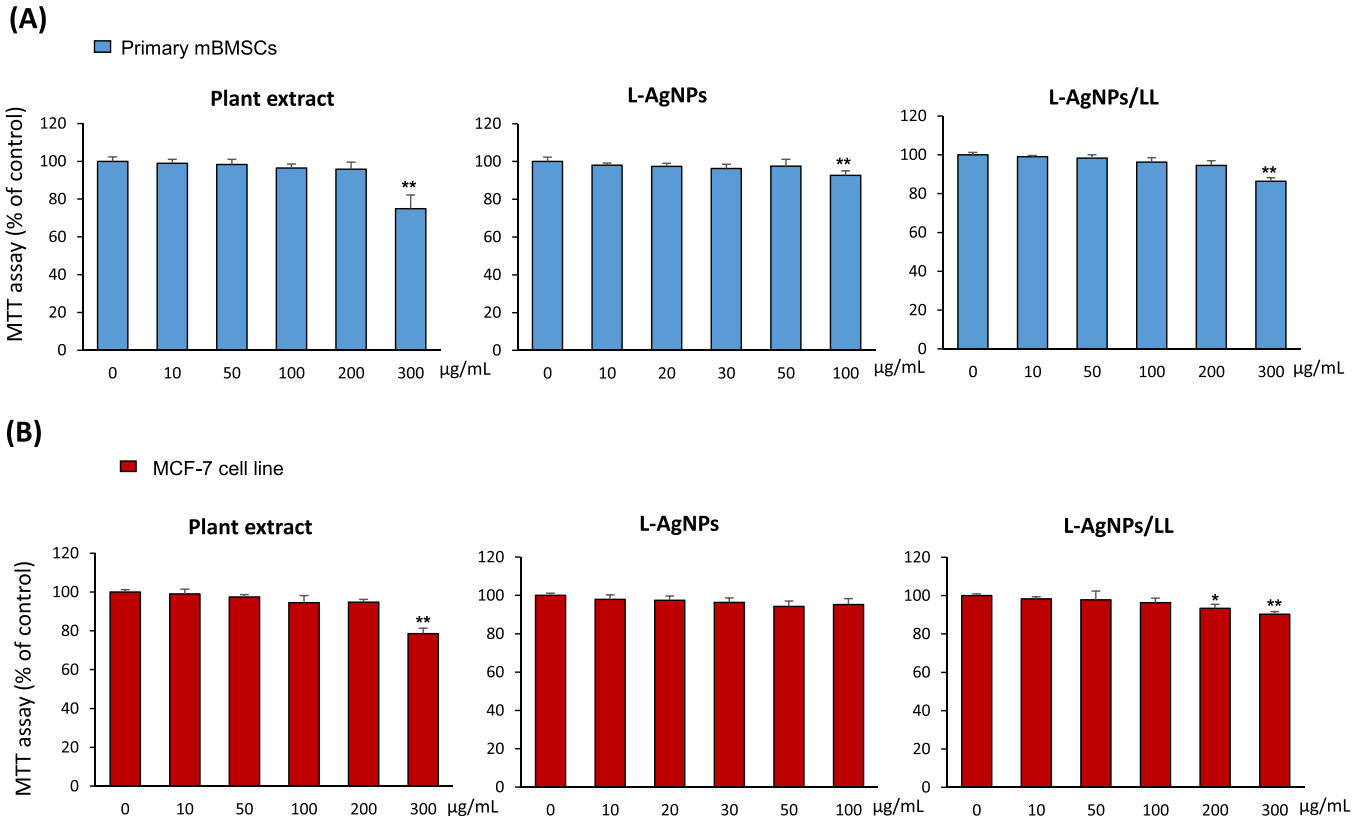

Figure 7. Cytotoxicity of the plant extract, L-AgNPs, and L-AgNPs/LL on the animal cell culture. (A) MTT assay was performed for primary isolated mBMSCs and (B) MCF-7 cell line treated with different concentrations of the plant extract, L-AgNPs, and L-AgNPs/LL after 48 h of treatment. Values are mean ± SD of three independent experiments (*$p < 0.05$, **$p < 0.005$ compared to control).

against *C. albicans*, *C. parapsilosis*, and *C. glabrata* with an MIC of 8 μg/mL,[37] while biosynthesized AgNPs using *Artemisia annua* showed MIC against *C. albicans*, *C. tropicalis*, and *C. glabrata* that ranged between 80 and 120 μg/mL. Furthermore, we have recently reported the anti-candidal action of AgNPs biosynthesized by the *Calotropis gigantea* leaf extract against *C. albicans* with an MIC of 50 μg/mL.[19] Thus, AgNPs produced by different approaches and species were reported to show antifungal activity at different MIC levels depending on their size, shape, and surface modification.[38−40]

Numerous mechanisms described the anti-candidal potential of AgNPs. These comprise the ability of AgNPs to destroy the membrane permeability and to damage the membrane lipid bilayers, leading to the leakage of ions, accompanied by formation of pores and dispersion of the membrane potential. Additionally, AgNPs were reported to block the cell cycle at the G2/M phase in *C. albicans*,[41] which, in turn, increases the production of reactive oxygen species (ROS), and decreases the metal-based antioxidant enzymes.[42]

https://dx.doi.org/10.1021/acsomega.0c06009
ACS Omega 2021, 6, 8151−8162

In this report, we investigated the efficacy of the antifungal potential of the combination therapy of L-AgNPs with the plant extract to provide a different approach for the effective control of *C. albicans*. Previously, the anti-candidal potential of AgNPs against *Candida* species was found to be enhanced using a combination with commercially available antifungal drugs such as fluconazole or amphotericin B.[43,44] Our data demonstrated that the antifungal action of AgNPs could be improved through the combination therapy of L-AgNPs with *L. lalambensis* extracts to deliver an innovative approach for the effective control of *C. albicans*. Thus, our results identified the *L. lalambensis* leaf extract as an alternative source of bioactive compounds that could contribute to the biosynthesis of AgNPs and has a powerful antifungal activity. Screening analysis of *L. lalambensis* extracts revealed the presence of several important secondary metabolites that could be responsible for the reduction and capping of AgNPs, such as lupeol, β-sitosterol, oleanolic acid, β-sitosterol glucoside, kaempferol, kaempferol-3-*O*-α-L-rhamnoside, and ethyl-*O*-β-D-glucopyranoside.[27] In addition, several phytochemicals with known antifungal activities were identified in *L. lalambensis* extracts[27,45] including flavonoids kaempferol,[46] rhamnosyl derivatives,[47,48] β-sitosterol,[49] and stigmasterol.[50] In this context, we have recently extracted and purified the phytochemical 5′-hydroxy auraptene (5′-HA) from *L. lalambensis* and demonstrated its antifungal activity.[28]

Our results showed the inhibitory effect of L-AgNPs/LL on the dimorphic transitions between yeast and filamentous forms. The dimorphic transitions between yeast and filamentous forms were identified as among the most important virulent attributes in *C. albicans*.[51] The formation of hyphae is a remarkable property of *C. albicans* that plays a key role in adherence and biofilm formation, which is definitely essential for colonization and pathogenesis of *C. albicans*.[52,53] Thus, the blocking of phenotypic switching from yeast to a hyphal form would mean controlling the infection. In this context, the biofabricated AgNPs using the aqueous leaf extract of *Polyalthia longifolia* were shown to target the Ras-mediated signal transduction pathways in *C. albicans* via downregulating the gene expression of the yeast-to-hyphal transition including the cell elongation gene (Ece1), hyphal inducer gene (Tec), and yeast-to-hyphal transition genes (Tup1 and Rfg1).[54]

Several studies confirmed the inhibitory effect of biosynthesized AgNPs alone on *C. albicans* biofilm formation.[39,55,56] Our data displayed the efficiency of L-AgNPs/LL to inhibit the adhesion and biofilm formation of *C. albicans*. Consistently, AgNPs biosynthesized using *Dodonaea viscosa* and *Hyptis suaveolens* leaf extracts strongly inhibited more than 80% of biofilm formed by *Candida* spp.[38] Similarly, the biosynthesized AgNPs using the aqueous extract of *Malva sylvestris* leaves showed significant anti-biofilm activity against *Candida* species.[57] The mechanism underlying the inhibition of biofilm formation using biosynthesized AgNPs includes the anti-adhesive potential of AgNPs, which regulates the growth of living microbial cells and the suppression of microbial adhesion gene expression.[58,59] Additionally, AgNPs inhibit blastospores and disrupt the cell walls of both the yeast and the hyphal forms in order to cause the suppression of biofilm formation in *Candida*.[55,56] In contrast to the plant extract alone, L-AgNPs/LL established an improved ability to disrupt fungal viability within mature biofilms. These can be attributed to enhanced permeation through the extracellular polymeric matrix released by biofilms.[60]

C. albicans established enzymatic antioxidant defense mechanisms in order to decrease the damaging actions of reactive oxygen species formed by phagocytes in the course of the infection process. Our results confirmed the inhibitory action of L-AgNPs/LL on the production of antioxidant enzymes by *C. albicans*. Phytochemicals from the *Lotus* genus were found to exert an antioxidant potential.[61] AgNPs were also described to exhibit antioxidant potential through the stimulation of *C. albicans* to express genes encoding for antioxidant enzymes, such as catalase, superoxide dismutase glutathione/glutaredoxin, glutathione peroxidase, and components of the thioredoxin systems.[42,62] The stimulatory action of AgNPs on oxidative stress as a mechanism of toxicity in *C. albicans* caused the shifting of the total redox balance to oxidation, therefore resulting in the functional destruction of cells.[63−65]

The release of glucose and trehalose is a consequence of the disruption of the cell membrane by L-AgNPs/LL. Our data showed that L-AgNPs- or plant-extract-treated cells accumulated more intracellular glucose and trehalose than the untreated cells. In this context, Kim et al. reported that extracellular glucose and trehalose of *C. albicans* induced by AgNPs were 30.3 μg per fungal dry weight of 1 mg, which is significantly higher than those of untreated cells.[41] Trehalose functions to interact with the phospholipids and other macromolecules on the cell membrane and thus protects pathogenic fungi against various stress conditions, such as desiccation, dehydration, heat, cold, oxidation, and toxic agents.[66,67] Trehalose can also shield the fungal cell membrane against dehydrated conditions via creating a glass state when there is no water retention or crystallization.[68]

Our results demonstrated that the treatment of *C. albicans* cells with L-AgNPs/LL resulted in significant modifications in the cell wall and membrane as examined by SEM and TEM. Consistently, major alterations in the surface appearance of *C. albicans* cells were reported for biosynthesized AgNP treatment.[56,69] These changes in the cell wall of treated *C. albicans* include a rough wrinkled outer cell wall, ruptured cell membrane, and dense cytoplasm without distinguished features. Such modifications could be triggered by the interference of AgNPs. Therefore, the mechanism of AgNPs on *C. albicans* may be attributed to the disruption of the cell wall and cell membrane, which displayed severe modifications to the cell wall causing blebs on the surface and cell collapse. Furthermore, AgNPs destroy the membrane permeability barrier via disturbing the membrane lipid bilayers leading to the leakage of ions and other materials along with formation of pores and dissipation of the electrical potential of the membrane.[41]

Our data demonstrated high cell survival (more than 95%) of both primary BMSCs and MCF7 cell line upon treatment with either L-AgNPs alone or in combination with the plant extract (L-AgNPs/LL) at MIC values. In support of this finding, biosynthesis of AgNPs using different plant extracts did not show cytotoxicity in human cells at MIC values.[19,70] The toxicity of AgNPs to human and animal cells was found to be related to the type of reducing agent used in the biosynthesis,[71] where surface chemistries of synthesized AgNPs using different reducing agents showed different cellular responses.[72] In this context, several studies demonstrated the non-cytotoxic effects of biosynthesized AgNPs on animal cells. For example, biosynthesized AgNPs using an ethanolic extract of fenugreek leaves showed low toxicity to the

https://dx.doi.org/10.1021/acsomega.0c06009
ACS Omega 2021, 6, 8151−8162

human skin cell line (HaCaT),[73] AgNPs synthesized by a cell-free culture filtrate of *Fusarium chlamydosporum* and *Penicillium chrysogenum* were nontoxic to human normal melanocytes (HFB 4),[74] and biosynthesized AgNPs using a leaf extract of *Calotropis gigantea* were nontoxic to BMSCs.[19] Additionally, the antioxidant and the anti-inflammatory activities of *Lotus* extracts might contribute toward reducing the cytotoxicity of AgNPs.[36,61] It is also possible that the plant extracts will act as a stabilizing agent to stabilize AgNPs against dissolution, consequently decreasing their toxicity. Thus, our study provides a combination of biosynthesized AgNPs and plant extract as a new safe model of formulation that can potentially be used in future drug development for oral candidiasis.

4. CONCLUSIONS

In this study, we biosynthesized AgNPs using the leaf extract of *L. lalambensis*. Our results demonstrated the effective anti-candidal potential of a combination of biosynthesized AgNPs and leaf extract of *L. lalambensis* (L-AgNPs/LL). L-AgNPs/LL significantly suppressed the growth, phenotypic switching, adhesion, biofilm formation, and the production of antioxidant defense enzymes by *C. albicans*. Additionally, L-AgNPs/LL displayed no sign of cytotoxicity at levels of MIC concentrations. Thus, L-AgNPs/LL provides a new approach for controlling the pathogenesis of *C. albicans* by inhibiting the main virulence attributes and development of biofilms. Further preclinical studies are required to assess the therapeutic potential of L-AgNPs/LL in the treatment of oral candidiasis *in vivo*.

5. EXPERIMENTAL SECTION

5.1. Collection of the Plant Material and Preparation of the Extract. *L. lalambensis* Schweinf was previously collected by our group,[29] from Eastern province, Al-Hassa, Saudi Arabia. The sample was identified taxonomically and authenticated by Dr. Monier Abd El-Ghani, Plant Taxonomy and Flora, the Herbarium, Department of Botany and Microbiology, Faculty of Science, Cairo University where a voucher specimen was deposited. The leaves were washed and allowed to dry at room temperature. The dried leaves were then crushed into fine powder. 50 g of leaf powder was added to 500 mL of distilled water, and the mixture was heated at 80 °C for 4 h with stirring. The resulting extract was filtered through Whatman filter paper no. 1 and stored at 4 °C for further use.

5.2. Biosynthesis of L-AgNPs. For each 50 mL of plant extract, a 10 mL solution of 1.699 mg/mL $AgNO_3$ was added to be transformed to AgNPs at 30 °C, and the mixture was heated at 80 °C for 3 h with stirring. The complete reduction was verified by a change in color from colorless to brown. The green biosynthesized AgNPs were separated by centrifugation at 15,000*g* for 30 min. The final green-synthesized AgNPs were denoted as L-AgNPs, freeze-dried, and stored at 4 °C for further experiments. UV−visible spectrophotometry (Santa Clara, CA, USA)[75] was used to verify the formation of L-AgNPs that presented surface plasmon resonance at 420 nm.

5.3. Characterization of AgNPs. *5.3.1. Transmission Electron Microscopy (TEM).* TEM was made following the method of Jalal et al.[76] on a Leo 912 AB instrument (Aalen, Germany). Concisely, a drop of the sample of L-AgNPs was decanted onto carbon-coated copper grids and left to stand for 2 min prior to imaging.

5.3.2. X-ray Diffraction Analysis (XRD). The lyophilized L-AgNPs coated on an XRD grid were exposed for XRD analysis. The measurement was made in an X-ray diffractometer supplied with an operating voltage of 45 kV, and the current was adjusted to 0.8 mA (Unisantis XMD-300, Geneva, Switzerland). The diffraction patterns were determined by Cu Kα radiation of wavelength 1.54 Å in the region of 2θ from 30 to 80°.[77]

5.3.3. Fourier Transform Infrared Spectroscopy (FTIR). The L-AgNPs were exposed for FTIR analysis (Thermo Nicolet AVATAR 370, Waltham, MA, USA) to study their spectra. The examination was performed by means of KBr pellets in the range of 500−4000 cm^{-1}.[77]

5.4. Anti-Candidal Activity of AgNPs. An oral species of *C. albicans* was kindly provided by the Micro-Analytical Center, Microbiology Laboratory, Faculty of Science, Cairo University and kept on Sabouraud dextrose agar (SDA) slopes at 4 °C. Inoculates were prepared from cultures on SDA slopes incubated at 37 °C for 16−18 h. The yeast cells were washed with sterile water, centrifuged, and suspended in water (under aseptic conditions). The anti-candidal activities of L- AgNPs and plant extract were measured as described previously.[78] The solution of L-AgNPs was prepared by dissolving L-AgNPs in 10% dimethyl sulfoxide (DMSO, 1000 μg/mL). The sample was sonicated for 20 min, and sterile filter paper disks containing 50 μg of L-AgNPs/disk were used. 10% DMSO was used as a negative control. The culture of *C. albicans* was diluted to 1×10^5 CFU, and the anti-candidal potential of the L-AgNPs and plant extract was determined by measuring their inhibition zone diameters after 48 h of incubation at 28 °C. The minimum inhibitory concentration (MIC) was determined by the bi-fold serial dilution method.[24] Different concentrations of L-AgNPs and plant extract (6.25−200 μg/mL) were used for the MIC assay. MIC values were expressed as μg/mL.

5.5. Synergistic Anti-Candidal Action of L-AgNPs/LL. The synergistic anti-candidal effects of L-AgNPs and plant extract mixture solution were determined against *C. albicans* as described previously.[19] For the preparation of L-AgNPs/LL, L-AgNPs (50 μg/mL) and plant extract (100 μg/mL) were mixed and sonicated for 15 min at room temperature. Paper disks were prepared by adding 50 μL of the L-AgNPs/LL mixture solution to 6 mm filter paper disks. MIC was evaluated by measuring the inhibition zone diameters.

5.6. Time-Kill Test. *C. albicans* was grown in RPMI-1640 with a starting inoculum of 10^5 CFU/mL. L-AgNPs, plant extract, and L-AgNPs/LL were added. At predetermined time points (0, 4, 8, 12, 16, 24, 36, and 48 h) after incubation with agitation at 30 °C, a 100 μL aliquot was removed from every solution and spread on a PDA plate. Colony counts were determined after incubation at 30 °C for 48 h.

5.7. Assay of *C. albicans* Hyphal Development in Liquid Media. *C. albicans* was grown in RPMI-1640 with a starting inoculum of 10^5 CFU/mL amended with L-AgNPs, plant extract, or L-AgNPs/LL at 37 °C for 24 h in a shaking incubator. A medium with 10% DMSO was used as a negative control. Aliquots of fungal cells were harvested after 24 h and observed in bright field with a Digital Cell Imaging System (Logos Bio Systems, Heidelberg, Germany).[79]

5.8. Adhesion and Biofilm Formation Assays. RPMI-1640 was inoculated with *C. albicans* (1×10^5 cells/mL) and then added to 96-well microtiter plates (Nunc, Roskilde, Denmark). DMSO, L-AgNPs, plant extract, and L-AgNPs/LL

https://dx.doi.org/10.1021/acsomega.0c06009
ACS Omega 2021, 6, 8151−8162

were added to *C. albicans* and incubated for 2 h for determination of adhesion and 24 h for determination of formation of the biofilm at 37 °C. Biofilm growth was determined by the MTT metabolic assay.[58] Wells without any antifungal agent were used as controls, while wells without biofilms were the blanks.

5.9. Determination of Antioxidant Enzymes. *C. albicans* was grown at 37 °C with L-AgNPs/LL. Cells were harvested and homogenized in homogenizing buffer (pH 7.5). The homogenate was centrifuged at 20,217*g* for 1 h at 4 °C. The supernatant was examined for protein concentration by the Lowry method,[80] and antioxidant enzyme activities were measured as follows.

5.9.1. Glutathione-S-transferases (GST). GST activity was determined spectrophotometrically by measuring glutathione (GSH) and 1-chloro-2,4-dinitrobenzene (CDNB) conjugate at 340 nm following the method of Habig et al.[81]

5.9.2. Catalase (CAT). Catalase activity was determined by measuring the decrease in absorbance of hydrogen peroxide at 240 nm following the method of Teranishi et al.[82]

5.9.3. Superoxide Dismutase (SOD). Superoxide dismutase activity was determined using the adrenochrome test that relies on the ability of SOD to inhibit the autoxidation of epinephrine in alkaline according to the method of McCord and Fridovich.[83]

5.9.4. Glutathione Reductase (GSR). Glutathione reductase activity was measured according to the method of Carlberg and Mannervik[84] in which one unit of glutathione reductase activity is defined as the amount of enzyme catalyzing the reduction of 1 μM NADPH per minute.

5.9.5. Glucose-6-phosphate Dehydrogenase (G6-P). Glucose-6-phosphate dehydrogenase activity was determined by measuring the reduction of NADP at 340 nm according to the method of Zaheer et al.[85]

5.10. Determination of Released Glucose and Trehalose. *C. albicans* were grown at 28 °C in a PDA medium. The cells were washed three times with PBS, and then 1 mL of the *C. albicans* suspension (1.0×10^6 CFU/mL), containing DMSO (negative control), L-AgNPs, plant extract, and L-AgNPs/LL, was incubated for 2 h at 28 °C in PBS. The fungal cells were precipitated by centrifugation (12,000 rpm for 20 min). Supernatants were mixed with 0.05 units of trehalase. The enzymatic reaction was carried out for 1 h at 37 °C, and then the reaction suspension was mixed with water and 16% DNS reagent (3,5-dinitrosalicylic acid 1%, NaOH 2%, sodium potassium tartrate 20%). For the reaction of glucose with the DNS reagent, the mixture was boiled for 5 min and allowed to cool. Color formations were measured at 525 nm.[41]

5.11. Ultrastructural Examination of *C. albicans* by SEM. Cells treated with L-AgNPs, plant extract, and L-AgNPs/LL were washed with PBS and fixed with 4% formaldehyde and 1% glutaraldehyde in PBS at room temperature. The samples were then rinsed twice with 0.1 M phosphate buffer and placed in 1% osmium tetroxide for 1 h. The drying of the samples was carried out in a series of ethanol. The samples were finally placed on copper grids to be observed by SEM using a Hitachi S-5500 (Hitachi High-Technologies Europe GmbH, Krefeld, Germany).[56]

5.12. Ultrastructural Examination of *C. albicans* Cells by TEM. A suspension of *C. albicans* cells (10^5 CFU/mL) prepared from yeast cultures grown for 24 h at 37 °C in PDA was mixed with L-AgNPs, plant extract, and L-AgNPs/LL. The samples were then centrifuged for 10 min at 3500 rpm. The resulting pellets were suspended in 5 mL of PBS and washed two times, and then the fungal cells were fixed by suspending each pellet in 1 mL of 4% formaldehyde and 1% glutaraldehyde in PBS. After 2 h of incubation at room temperature, the samples were stored at 4 °C and stained with 1% osmium tetroxide. The *Candida* cells were then washed with PBS, dehydrated with a series of ethanol, fixed in a resin, and allowed to solidify for 48 h at 60 °C. The resin capsules were cut using a Porter Blum MT-2 ultra-microtome (Sorval, Liverpool, NY, USA). Ultrathin sections were obtained and examined by TEM using a JEM-ARM200F (JEOL USA Inc., MA, USA).[86]

5.13. Cell Culture and Cytotoxicity Assay. Primary mouse bone marrow derived mesenchymal stem cells (BMSCs) were isolated from 8 week old male C57BL/6J mice according to our previously described protocols.[87] Briefly, whole bone marrow cells were flushed out from mouse tibia and femur and centrifuged in 1 mL Eppendorf tubes for 1 min at 400*g*. Cells were suspended in PBS, filtered through a 70 μm filter, and cultured in 60 cm^2 Petri dish in an RPMI-1640 medium supplemented with 1% penicillin/streptomycin (P/S) (Gibco Invitrogen, USA) and 12% FBS (Gibco Invitrogen, USA). Cells were cultured in a 5% CO_2 incubator at 37 °C for 24 h, and nonadherent cells were collected by centrifugation and cultured in a fresh medium. BMSCs were continued to be subcultured at a split ratio of 1:2. The human breast adenocarcinoma MCF-7 cell line (ACC 115, Braunschweig, Germany) was cultured in DMEM supplemented with 10% FBS, 10 μg/mL insulin (Gibco Invitrogen, USA), and 1% penicillin/streptomycin (P/S).

For the cytotoxicity assay, cell viability was measured using the MTT cell proliferation assay kit (Sigma-Aldrich) according to the manufacturer's instruction kit. Cells were treated with L-AgNPs, plant extract, or L-AgNPs/LL at different concentrations in 96-well plates for 48 h. Cells were then incubated with a medium containing 0.5 mg/mL MTT to metabolize to formazan. Optical density was measured at 550 nm using an ELISA plate reader.[29] The values of cell viability were presented as percentage of control, DMSO-treated cells.

5.14. Statistical Analysis. All values are expressed as mean ± SD (standard deviation) of at least three independent experiments. Power calculation was performed for 2-samples using unpaired Student's *t* test (2-tailed) assuming equal variation in the two groups. Differences were considered statistically significant at $^*P < 0.05$ and $^{**}P < 0.005$.

AUTHOR INFORMATION

Corresponding Author

Basem M. Abdallah − *Department of Biological Sciences, College of Science, King Faisal University, Al-Ahsa 31982, Saudi Arabia; Endocrine Research (KMEB), Department of Endocrinology, University of Southern Denmark, Odense DK-5000, Denmark;* orcid.org/0000-0003-0324-8055; Phone: +966(013)5899430; Email: babdallallah@kfu.edu.sa

Author

Enas M. Ali − *Department of Biological Sciences, College of Science, King Faisal University, Al-Ahsa 31982, Saudi Arabia; Department of Botany and Microbiology, Faculty of Science, Cairo University, Cairo 12613, Egypt*

Complete contact information is available at: https://pubs.acs.org/10.1021/acsomega.0c06009

https://dx.doi.org/10.1021/acsomega.0c06009
ACS Omega 2021, 6, 8151−8162

Author Contributions

B.M.A. and E.M.A. conceived the project, designed the study, performed the experiments, analyzed the data, and edited the manuscript. E.M.A. wrote the first draft of the manuscript.

Notes

The authors declare no competing financial interest.
All materials are available from the corresponding author.

■ ACKNOWLEDGMENTS

The authors extend their appreciation to the Deputyship of Research & Innovation, Ministry of Education in Saudi Arabia for funding this research work through the project number IFT 20029.

■ REFERENCES

(1) Wade, W. G. The oral microbiome in health and disease. *Pharmacol. Res.* **2013**, *69*, 137−143.
(2) Harpf, V.; Rambach, G.; Würzner, R.; Lass-Flörl, C.; Speth, C. Candida and Complement: New Aspects in an Old Battle. *Front. Immunol.* **2020**, *11*, 1471.
(3) Edelmann, A.; Kruger, M.; Schmid, J. Genetic relationship between human and animal isolates of Candida albicans. *J. Clin. Microbiol.* **2005**, *43*, 6164−6166.
(4) Dadar, M.; Tiwari, R.; Karthik, K.; Chakraborty, S.; Shahali, Y.; Dhama, K. Candida albicans - Biology, molecular characterization, pathogenicity, and advances in diagnosis and control - An update. *Microb. Pathog.* **2018**, *117*, 128−138.
(5) Castelo-Branco, D. S. C. M.; Brilhante, R. S. N.; Paiva, M. A. N.; Teixeira, C. E. C.; Caetano, E. P.; Ribeiro, J. F.; Cordeiro, R. A.; Sidrim, J. J. C.; Monteiro, A. J.; Rocha, M. F. G. Azole-resistant Candida albicans from a wild Brazilian porcupine (Coendou prehensilis): a sign of an environmental imbalance? *Med. Mycol.* **2013**, *51*, 555−560.
(6) Lamm, C. G.; Love, B. C.; Rodgers, L. L.; Campbell, G. A. Pathology in practice. Fungal dermatitis in a camel caused by Candida albicans. *J. Am. Vet. Med. Association* **2009**, *234*, 1013−1015.
(7) Mueller, R. S.; Bettenay, S. V.; Shipstone, M. Cutaneous candidiasis in a dog caused by Candida guilliermondii. *Vet. Rec.* **2002**, *150*, 728−730.
(8) Böhme, A.; Karthaus, M.; Hoelzer, D. Antifungal prophylaxis in neutropenic patients with hematologic malignancies. *Antibiot. Chemother.* **2000**, *50*, 69−78.
(9) Silva, S.; Rodrigues, C.; Araújo, D.; Rodrigues, M.; Henriques, M. Candida Species Biofilms' Antifungal Resistance. *J. Fungi (Basel)* **2017**, *3*, 8.
(10) Jose, A.; Coco, B. J.; Milligan, S.; Young, B.; Lappin, D. F.; Bagg, J.; Murray, C.; Ramage, G. Reducing the incidence of denture stomatitis: are denture cleansers sufficient? *J. Prosthodont.* **2010**, *19*, 252−257.
(11) Gimble, J. M.; Zvonic, S.; Floyd, Z. E.; Kassem, M.; Nuttall, M. E. Playing with bone and fat. *J. Cell. Biochem.* **2006**, *98*, 251−266.
(12) McKeny, P. T.; Nessel, T. A.; Zito, P. M. Antifungal Antibiotics. In *StatPearls*, StatPearls Publishing, StatPearls Publishing LLC.: Treasure Island (FL), 2020.
(13) Bona, E.; Cantamessa, S.; Pavan, M.; Novello, G.; Massa, N.; Rocchetti, A.; Berta, G.; Gamalero, E. Sensitivity of Candida albicans to essential oils: are they an alternative to antifungal agents? *J. Appl. Microbiol.* **2016**, *121*, 1530−1545.
(14) Giordani, R.; Regli, P.; Kaloustian, J.; Mikaïl, C.; Abou, L.; Portugal, H. Antifungal effect of various essential oils against Candida albicans. Potentiation of antifungal action of amphotericin B by essential oil from Thymus vulgaris. *Phytother. Res.* **2004**, *18*, 990−995.
(15) Hammer, K. A.; Carson, C. F.; Riley, T. V. Antifungal effects of Melaleuca alternifolia (tea tree) oil and its components on Candida albicans, Candida glabrata and Saccharomyces cerevisiae. *J. Antimicrob. Chemother.* **2004**, *53*, 1081−1085.
(16) Souza, M. E.; Lopes, L. Q. S.; Bonez, P. C.; Gündel, A.; Martinez, D. S. T.; Sagrillo, M. R.; Giongo, J. L.; Vaucher, R. A.; Raffin, R. P.; Boligon, A. A.; Santos, R. C. V. Melaleuca alternifolia nanoparticles against Candida species biofilms. *Microb. Pathog.* **2017**, *104*, 125−132.
(17) Lee, S.; Jun, B.-H. Silver Nanoparticles: Synthesis and Application for Nanomedicine. *Int. J. Mol. Sci.* **2019**, *20*, 865.
(18) Żarowska, B.; Koźlecki, T.; Piegza, M.; Jaros-Koźlecka, K.; Robak, M. New Look on Antifungal Activity of Silver Nanoparticles (AgNPs). *Pol. J. Microbiol.* **2019**, *68*, 515−525.
(19) Ali, E. M.; Abdallah, B. M. Effective Inhibition of Candidiasis Using an Eco-Friendly Leaf Extract of Calotropis-gigantean-Mediated Silver Nanoparticles. *Nanomaterials (Basel, Switzerland)* **2020**, *10*, 422.
(20) Siddiqi, K. S.; Husen, A.; Rao, R. A. K. A review on biosynthesis of silver nanoparticles and their biocidal properties. *J. Nanobiotechnology* **2018**, *16*, 14.
(21) Govender, R.; Phulukdaree, A.; Gengan, R. M.; Anand, K.; Chuturgoon, A. A. Silver nanoparticles of Albizia adianthifolia: the induction of apoptosis in human lung carcinoma cell line. *J. Nanobiotechnology* **2013**, *11*, 5.
(22) Ovais, M.; Khalil, A. T.; Raza, A.; Khan, M. A.; Ahmad, I.; Islam, N. U.; Saravanan, M.; Ubaid, M. F.; Ali, M.; Shinwari, Z. K. Green synthesis of silver nanoparticles via plant extracts: beginning a new era in cancer theranostics. *Nanomedicine (Lond.)* **2016**, *11*, 3157−3177.
(23) El-Moslamy, S. H.; Elkady, M. F.; Rezk, A. H.; Abdel-Fattah, Y. R. Applying Taguchi design and large-scale strategy for mycosynthesis of nano-silver from endophytic Trichoderma harzianum SYA.F4 and its application against phytopathogens. *Sci. Rep.* **2017**, *7*, 45297.
(24) Abbasi, E.; Milani, M.; Fekri Aval, S.; Kouhi, M.; Akbarzadeh, A.; Tayefi Nasrabadi, H.; Nikasa, P.; Joo, S. W.; Hanifehpour, Y.; Nejati-Koshki, K.; Samiei, M. Silver nanoparticles: Synthesis methods, bio-applications and properties. *Crit. Rev. Microbiol.* **2016**, *42*, 173−180.
(25) el-Mousallami, A. M. D.; Afifi, M. S.; Hussein, S. A. M. Acylated flavonol diglucosides from Lotus polyphyllos. *Phytochemistry* **2002**, *60*, 807−811.
(26) Mahasneh, A. M. Screening of some indigenous Qatari medicinal plants for antimicrobial activity. *Phytother. Res.* **2002**, *16*, 751−753.
(27) Al-Youssef, H.; Murphy, B.; Amer, M.; Abdel-Kader, M.; Kingston, D. Phytochemical and biological study of the aerial parts of Lotus lalambensis growing in Saudi Arabia. *Saudi Pharm J.* **2008**, *16*, 122.
(28) Ali, E. M.; Alkuwayti, M. A.; Aldayel, M. F.; Abdallah, B. M. Coumarin derivative, 5′-hydroxy-auraptene, extracted from Lotus lalambensis, displays antifungal and anti-aflatoxigenic activities against Aspergillus flavus. *J. King Saud Univ. - Sci.* **2020**, 101216.
(29) Abdallah, B. M.; Ali, E. M. 5′-hydroxy Auraptene stimulates osteoblast differentiation of bone marrow-derived mesenchymal stem cells via a BMP-dependent mechanism. *J. Biomed. Sci.* **2019**, *26*, 51.
(30) Abdallah, B. M.; Ali, E. M.; Elsawy, H.; Badr, G. M.; Abdel-Moneim, A. M.; Alzahrani, A. M. The Coumarin Derivative 5'-Hydroxy Auraptene Suppresses Osteoclast Differentiation via Inhibiting MAPK and c-Fos/NFATc1 Pathways. *Biomed. Res. Int.* **2019**, *2019*, 9395146.
(31) Henglein, A. Physicochemical properties of small metal particles in solution: "microelectrode" reactions, chemisorption, composite metal particles, and the atom-to-metal transition. *J. Phys. Chem.* **1993**, *97*, 5457−5471.
(32) Sastry, M.; Patil, V.; Sainkar, S. R. Electrostatically Controlled Diffusion of Carboxylic Acid Derivatized Silver Colloidal Particles in Thermally Evaporated Fatty Amine Films. *J. Phys. Chem. B* **1998**, *102*, 1404−1410.
(33) Pal, S.; Tak, Y. K.; Song, J. M. Does the antibacterial activity of silver nanoparticles depend on the shape of the nanoparticle? A study of the Gram-negative bacterium Escherichia coli. *Appl. Environ. Microbiol.* **2007**, *73*, 1712−1720.

https://dx.doi.org/10.1021/acsomega.0c06009
ACS Omega 2021, 6, 8151−8162

(34) Nazeruddin, G. M.; Prasad, N. R.; Prasad, S. R.; Shaikh, Y. I.; Waghmare, S. R.; Adhyapak, P. Coriandrum sativum seed extract assisted in situ green synthesis of silver nanoparticle and its antimicrobial activity. *Industrial Crops and Products* **2014**, *60*, 212−216.
(35) Basavaraja, S.; Balaji, S. D.; Lagashetty, A.; Rajasab, A. H.; Venkataraman, A. Extracellular biosynthesis of silver nanoparticles using the fungus Fusarium semitectum. *Mater. Res. Bull.* **2008**, *43*, 1164−1170.
(36) Girardi, F. A.; Tonial, F.; Chini, S. O.; Sobottka, A. M.; Scheffer-Basso, S. M.; Bertol, C. D. Phytochemical profile and antimicrobial properties of Lotus spp. (Fabaceae). *An. Acad. Bras. Cienc.* **2014**, *86*, 1295−1302.
(37) Choi, J. S.; Lee, J. W.; Shin, U. C.; Lee, M. W.; Kim, D. J.; Kim, S. W. Inhibitory Activity of Silver Nanoparticles Synthesized Using Lycopersicon Esculentum against Biofilm Formation in Candida Species. *Nanomaterials (Basel)* **2019**, *9*, 1512.
(38) Muthamil, S.; Devi, V. A.; Balasubramaniam, B.; Balamurugan, K.; Pandian, S. K. Green synthesized silver nanoparticles demonstrating enhanced in vitro and in vivo antibiofilm activity against Candida spp. *J. Basic Microbiol.* **2018**, *58*, 343−357.
(39) Jalal, M.; Ansari, M. A.; Alzohairy, M. A.; Ali, S. G.; Khan, H. M.; Almatroudi, A.; Siddiqui, M. I. Anticandidal activity of biosynthesized silver nanoparticles: effect on growth, cell morphology, and key virulence attributes of Candida species. *Int. J. Nanomed.* **2019**, *Volume 14*, 4667−4679.
(40) Monteiro, D. R.; Silva, S.; Negri, M.; Gorup, L. F.; de Camargo, E. R.; Oliveira, R.; Barbosa, D. B.; Henriques, M. Silver colloidal nanoparticles: effect on matrix composition and structure of Candida albicans and Candida glabrata biofilms. *J. Appl. Microbiol.* **2013**, *114*, 1175−1183.
(41) Kim, K. J.; Sung, W. S.; Suh, B. K.; Moon, S. K.; Choi, J. S.; Kim, J. G.; Lee, D. G. Antifungal activity and mode of action of silver nano-particles on Candida albicans. *BioMetals* **2009**, *22*, 235−242.
(42) Dantas, A.; Day, A.; Ikeh, M.; Kos, I.; Achan, B.; Quinn, J. Oxidative stress responses in the human fungal pathogen, Candida albicans. *Biomolecules* **2015**, *5*, 142−165.
(43) Longhi, C.; Santos, J. P.; Morey, A. T.; Marcato, P. D.; Durán, N.; Pinge-Filho, P.; Nakazato, G.; Yamada-Ogatta, S. F.; Yamauchi, L. M. Combination of fluconazole with silver nanoparticles produced by Fusarium oxysporum improves antifungal effect against planktonic cells and biofilm of drug-resistant Candida albicans. *Med. Mycol.* **2016**, *54*, 428−432.
(44) Ahmad, A.; Wei, Y.; Syed, F.; Tahir, K.; Taj, R.; Khan, A. U.; Hameed, M. U.; Yuan, Q. Amphotericin B-conjugated biogenic silver nanoparticles as an innovative strategy for fungal infections. *Microb. Pathog.* **2016**, *99*, 271−281.
(45) Al-Youssef, H.; Murphy, B. T.; Amer, M.; Al-Rehaily, A. J.; Abdel-Kader, M.; Kingston, D. Two new flavonol glycosides from the aerial parts of Lotus lalambensis growing in Saudi Arabia. *Nat. Prod. Sci.* **2008**, *14*, 86−89.
(46) Rocha, M. F. G.; Sales, J. A.; da Rocha, M. G.; Galdino, L. M.; de Aguiar, L.; de Aquino Pereira-Neto, W.; de Aguiar Cordeiro, R.; Castelo-Branco, D.; Sidrim, J. J. C.; Brilhante, R. S. N. Antifungal effects of the flavonoids kaempferol and quercetin: a possible alternative for the control of fungal biofilms. *Biofouling* **2019**, *35*, 320−328.
(47) Matin, M. M.; Ibrahim, M.; Rahman, M. S. Antimicrobial evaluation of methyl 4-O-acetyl-α-L-rhamnopyranoside derivatives. *Chittagong Univ. J. Biol. Sci.* **2008**, *3*, 33−43.
(48) Matin, M.; Nath, A.; Saad, O.; Bhuiyan, M.; Kadir, F.; Hamid, S. A.; Alhadi, A.; Ali, M.; Yehye, W. Synthesis, PASS-Predication and in Vitro Antimicrobial Activity of Benzyl 4-O-benzoyl-α-l-rhamnopyranoside Derivatives. *Int. J. Mol. Sci.* **2016**, *17*, 1412.
(49) Kiprono, P. C.; Kaberia, F.; Keriko, J. M.; Karanja, J. N. The in vitro anti-fungal and anti-bacterial activities of beta-sitosterol from Senecio lyratus (Asteraceae). *Z. Naturforschung C. J. of Biosci.* **2000**, *55*, 485−488.
(50) Mbambo, B.; Odhav, B.; Mohanlall, V. Antifungal activity of stigmasterol, sitosterol and ergosterol from Bulbine natalensis Baker (Asphodelaceae). *J. Med. Plant Res.* **2012**, *6*, 5135−5141.
(51) Peters, B. M.; Palmer, G. E.; Nash, A. K.; Lilly, E. A.; Fidel, P. L., Jr.; Noverr, M. C. Fungal morphogenetic pathways are required for the hallmark inflammatory response during Candida albicans vaginitis. *Infect. Immun.* **2014**, *82*, 532−543.
(52) Carradori, S.; Chimenti, P.; Fazzari, M.; Granese, A.; Angiolella, L. Antimicrobial activity, synergism and inhibition of germ tube formation by Crocus sativus-derived compounds against Candida spp. *J. Enzyme Inhib. Med. Chem.* **2016**, *31*, 189−193.
(53) Modrzewska, B.; Kurnatowski, P. Adherence of Candida sp. to host tissues and cells as one of its pathogenicity features. *Ann. Parasitol.* **2015**, *61*, 3−9.
(54) Halbandge, S. D.; Jadhav, A. K.; Jangid, P. M.; Shelar, A. V.; Patil, R. H.; Karuppayil, S. M. Molecular targets of biofabricated silver nanoparticles in Candida albicans. *J. Antibiot.* **2019**, *72*, 640−644.
(55) Różalska, B.; Sadowska, B.; Budzyńska, A.; Bernat, P.; Różalska, S. Biogenic nanosilver synthesized in Metarhizium robertsii waste mycelium extract - As a modulator of Candida albicans morphogenesis, membrane lipidome and biofilm. *PLoS One* **2018**, *13*, No. e0194254.
(56) Lara, H. H.; Romero-Urbina, D. G.; Pierce, C.; Lopez-Ribot, J. L.; Arellano-Jiménez, M. J.; Jose-Yacaman, M. Effect of silver nanoparticles on Candida albicans biofilms: an ultrastructural study. *J. Nanobiotechnology* **2015**, *13*, 91.
(57) Feizi, S.; Taghipour, E.; Ghadam, P.; Mohammadi, P. Antifungal, antibacterial, antibiofilm and colorimetric sensing of toxic metals activities of eco friendly, economical synthesized Ag/AgCl nanoparticles using Malva Sylvestris leaf extracts. *Microb. Pathog.* **2018**, *125*, 33−42.
(58) Vazquez-Muñoz, R.; Avalos-Borja, M.; Castro-Longoria, E. Ultrastructural analysis of Candida albicans when exposed to silver nanoparticles. *PLoS One* **2014**, *9*, No. e108876.
(59) Gulati, M.; Nobile, C. J. Candida albicans biofilms: development, regulation, and molecular mechanisms. *Microbes Infect.* **2016**, *18*, 310−321.
(60) Sanchez, D. A.; Schairer, D.; Tuckman-Vernon, C.; Chouake, J.; Kutner, A.; Makdisi, J.; Friedman, J. M.; Nosanchuk, J. D.; Friedman, A. J. Amphotericin B releasing nanoparticle topical treatment of Candida spp. in the setting of a burn wound. *Nanomedicine* **2014**, *10*, 269−277.
(61) Youssef, A.; El-Swaify, Z.; Maaty, D.; Youssef, M.; Garrido, G. Comparative study of two Lotus species: Phytochemistry, cytotoxicity and antioxidant capacity. *J. Pharm. Pharmacogn. Res.* **2020**, *8*, 537−548.
(62) Zhang, X. F.; Liu, Z. G.; Shen, W.; Gurunathan, S. Silver Nanoparticles: Synthesis, Characterization, Properties, Applications, and Therapeutic Approaches. *Int. J. of Mol. Sci.* **2016**, *17*, 1534.
(63) Arora, S.; Jain, J.; Rajwade, J. M.; Paknikar, K. M. Cellular responses induced by silver nanoparticles: In vitro studies. *Toxicol. Lett.* **2008**, *179*, 93−100.
(64) Liao, S.; Zhang, Y.; Pan, X.; Zhu, F.; Jiang, C.; Liu, Q.; Cheng, Z.; Dai, G.; Wu, G.; Wang, L.; Chen, L. Antibacterial activity and mechanism of silver nanoparticles against multidrug-resistant Pseudomonas aeruginosa. *Int. J. Nanomed.* **2019**, *Volume 14*, 1469−1487.
(65) Yuan, Y. G.; Peng, Q. L.; Gurunathan, S. Effects of Silver Nanoparticles on Multiple Drug-Resistant Strains of Staphylococcus aureus and Pseudomonas aeruginosa from Mastitis-Infected Goats: An Alternative Approach for Antimicrobial Therapy. *Int. J. Mol. Sci.* **2017**, *18*, 569.
(66) Alvarez-Peral, F. J.; Zaragoza, O.; Pedreno, Y.; Argüelles, J. C. Protective role of trehalose during severe oxidative stress caused by hydrogen peroxide and the adaptive oxidative stress response in Candida albicans. *Microbiology* **2002**, *148*, 2599−2606.
(67) Miao, Y.; Tenor, J. L.; Toffaletti, D. L.; Washington, E. J.; Liu, J.; Shadrick, W. R.; Schumacher, M. A.; Lee, R. E.; Perfect, J. R.; Brennan, R. G. Structures of trehalose-6-phosphate phosphatase from

https://dx.doi.org/10.1021/acsomega.0c06009
ACS Omega 2021, 6, 8151−8162

pathogenic fungi reveal the mechanisms of substrate recognition and catalysis. *Proc. Natl. Acad. Sci. U. S. A.* **2016**, *113*, 7148−7153.
(68) Zheng, Y. H.; Ma, Y. Y.; Ding, Y.; Chen, X. Q.; Gao, G. X. An insight into new strategies to combat antifungal drug resistance. *Drug Des. Devel. Ther.* **2018**, *Volume 12*, 3807−3816.
(69) Radhakrishnan, V. S.; Reddy Mudiam, M. K.; Kumar, M.; Dwivedi, S. P.; Singh, S. P.; Prasad, T. Silver nanoparticles induced alterations in multiple cellular targets, which are critical for drug susceptibilities and pathogenicity in fungal pathogen (Candida albicans). *Int. J. Nanomed.* **2018**, *Volume 13*, 2647−2663.
(70) Alsalhi, M.; Devanesan, S.; Alfuraydi, A.; Vishnubalaji, R.; Munusamy, M. A.; Murugan, K.; Nicoletti, M.; Benelli, G. Green synthesis of silver nanoparticles using Pimpinella anisum seeds: antimicrobial activity and cytotoxicity on human neonatal skin stromal cells and colon cancer cells. *Int. J. Nanomed.* **2016**, *Volume 11*, 4439−4449.
(71) Marin, S.; Vlasceanu, G.; Tiplea, R.; Bucur, I.; Lemnaru, M.; Marin, M.; Grumezescu, A. Applications and toxicity of silver nanoparticles: a recent review. *Curr. Top. Med. Chem.* **2015**, *15*, 1596−1604.
(72) Sur, I.; Altunbek, M.; Kahraman, M.; Culha, M. The influence of the surface chemistry of silver nanoparticles on cell death. *Nanotechnology* **2012**, *23*, 375102.
(73) Senthil, B.; Devasena, T.; Prakash, B.; Rajasekar, A. Non-cytotoxic effect of green synthesized silver nanoparticles and its antibacterial activity. *J. Photochem. Photobiol. B.* **2017**, *177*, 1−7.
(74) Khalil, N. M.; Abd El-Ghany, M. N.; Rodríguez-Couto, S. Antifungal and anti-mycotoxin efficacy of biogenic silver nanoparticles produced by Fusarium chlamydosporum and Penicillium chrysogenum at non-cytotoxic doses. *Chemosphere* **2019**, *218*, 477−486.
(75) Banerjee, P.; Satapathy, M.; Mukhopahayay, A.; Das, P. Leaf extract mediated green synthesis of silver nanoparticles from widely available Indian plants: synthesis, characterization, antimicrobial property and toxicity analysis. *Bioresour. Bioprocess.* **2014**, *1*, 3.
(76) Jalal, M.; Ansari, M. A.; Shukla, A. K.; Ali, S. G.; Khan, H. M.; Pal, R.; Alam, J.; Cameotra, S. S. Green synthesis and antifungal activity of Al2O3 NPs against fluconazole-resistant Candida spp isolated from a tertiary care hospital. *RSC Adv.* **2016**, *6*, 107577−107590.
(77) Bahrami-Teimoori, B.; Nikparast, Y.; Hojatianfar, M.; Akhlaghi, M.; Ghorbani, R.; Pourianfar, H. R. Characterisation and antifungal activity of silver nanoparticles biologically synthesised by Amaranthus retroflexus leaf extract. *J. Exp. Nanosci.* **2017**, *12*, 129−139.
(78) Patra, J. K.; Baek, K. H. Antibacterial Activity and Synergistic Antibacterial Potential of Biosynthesized Silver Nanoparticles against Foodborne Pathogenic Bacteria along with its Anticandidal and Antioxidant Effects. *Front. Microbiol.* **2017**, *08*, 167.
(79) Manoharan, R. K.; Lee, J. H.; Kim, Y. G.; Lee, J. Alizarin and Chrysazin Inhibit Biofilm and Hyphal Formation by Candida albicans. *Front. cell. Infect. Microbiol.* **2017**, *7*, 447.
(80) Lowry, O. H.; Rosebrough, N. J.; Farr, A. L.; Randall, R. J. Protein measurement with the Folin phenol reagent. *The Journal of biological chemistry* **1951**, *193*, 265−275.
(81) Habig, W. H.; Pabst, M. J.; Jakoby, W. B. Glutathione S-transferases. The first enzymatic step in mercapturic acid formation. *J. Biol. Chem.* **1974**, *249*, 7130−7139.
(82) Teranishi, Y.; Tanaka, A.; Osumi, M.; Fukui, S. Catalase Activities of Hydrocarbon-utilizing Candida Yeasts. *Agric. Biol. Chem.* **1974**, *38*, 1213−1220.
(83) McCord, J. M.; Fridovich, I. Superoxide dismutase. An enzymic function for erythrocuprein (hemocuprein). *J. Biol. Chem.* **1969**, *244*, 6049−6055.
(84) Carlberg, I.; Mannervik, B. Glutathione reductase. *Methods Enzymol.* **1985**, *113*, 484−490.
(85) Zaheer, N.; Tewari, K. K.; Krishnan, P. S. Mitochondrial forms of glucose 6-phosphate dehydrogenase and 6-phosphogluconic acid dehydrogenase in rat liver. *Arch. Biochem. Biophys.* **1967**, *120*, 22−34.
(86) Shinobu-Mesquita, C.; Bonfim-Mendonça, P.; Moreira, A.; Ferreira, I.; Donatti, L.; Fiorini, A.; Svidzinski, T. Cellular Structural Changes in Candida albicans Caused by the Hydroalcoholic Extract from Sapindus saponaria L. *Molecules* **2015**, *20*, 9405−9418.
(87) Abdallah, B. M.; Alzahrani, A. M.; Abdel-Moneim, A. M.; Ditzel, N.; Kassem, M. A simple and reliable protocol for long-term culture of murine bone marrow stromal (mesenchymal) stem cells that retained their in vitro and in vivo stemness in long-term culture. *Biol. proced. Online* **2019**, *21*, 3.

https://dx.doi.org/10.1021/acsomega.0c06009
ACS Omega 2021, 6, 8151−8162